Robotica: (2021) volume 39, pp. 1468–1484. © The Author(s), 2021. Published by Cambridge University Press.
doi:10.1017/S0263574720001289

Dynamic Modeling and Optimal Control of a Novel Microswimmer with Gimbal Based Disks

Ali Nickandish and Hossein Nejat Pishkenari*

Nano Robotics Laboratory, Department of Mechanical Engineering, Sharif University of Technology, Tehran, Iran

(Accepted December 4, 2020. First published online: January 8, 2021)

SUMMARY
We have introduced a new low-Reynolds-number microrobot with high 3D maneuverability. Our novel proposed microrobot has a higher rank of the controllability matrix with respect to the previous microswimmers which makes it capable of performing complex motions in space. In this study, governing equations of the microswimmer's motion have been derived and simulated. Subsequently, we have proposed a cascade optimal control technique to control the swimmer trajectory. In the proposed control scheme, the actuation is provided in a way that an exponential stability on the system trajectory error as well as minimum fluctuations of control signals are achieved.

KEYWORDS: Low-Reynolds-number swimmer; Microswimmer; Dynamic modeling; Microrobot; Control.

1. Introduction

Microrobots can be utilized for non-invasive medical treatments. They are an appropriate choice for in vivo applications such as diagnosis and therapeutic procedures. For example, a swimmer with a helical tail and a magnetic head can swim controllably through a vessel and clear blood clots.[1] This type of swimmers also can be used for cellular cargo delivery like assisted fertilization by carrying a sperm.[2] Using microrobots for treating has a big advantage over common therapy methods due to their low side effects.[3]

In studying the movement of immersed bodies, the Reynolds number is a significant factor. The Reynolds number is a ratio between inertial and viscous forces on an immersed body. When the Reynolds number is small, viscous forces play the main role in driving the objects. Since in the low-Reynolds-number condition the inertial terms can be neglected, in this condition the Navier–Stokes equation can be replaced by the Stokes equation as follows:

$$-\nabla p + \mu \nabla^2 \boldsymbol{v} = 0 \tag{1}$$

where p is the pressure, $\boldsymbol{v}$ is the velocity and μ is the viscosity of the fluid. In Eq. (1), the time effect is negligible and the flow pattern around the object does not depend on its speed. Thus, reciprocal movements do not lead to the swimmer displacement in space. Therefore, the time symmetry has to be broken for stroking and this happens with a swimmer which has at least two degrees of freedom.[4] In other words, the time independency and linearity of the Stokes equation in low-Reynolds-number condition define two noteworthy properties. First of all, the swimmer motion is independent of the actuation rate. For instance, there is no difference between the distances which a swimmer travels with fast and low-speed actuation. Secondly, if the deformations of a swimmer are reciprocal motion,

* Corresponding author. E-mail: nejat@sharif.edu

https://doi.org/10.1017/S0263574720001289 Published online by Cambridge University Press

then the average translation is zero. This property is expressed in the scallop theorem. For controlling a swimmer in low Reynolds, the second property is a geometry constraint and should be noticed.[5]

There are numerous applications for artificial low-Reynolds-number swimmers. For instance, they are useful in medical applications, such as delivering drugs to the specific cells, navigating through the body to find and cure the disease with minimum side effects. The low-Reynolds-number swimmers are not limited to the micro-scales. Even in macro-scales, they are applicable. As an example, they could be used for inspection of a highly viscous reservoir.

Najafi and Golestanian introduced a simple low-Reynolds-number swimmer consisting of three spheres and two linear actuators.[6] The Najafi–Golestanian microsimmer was studied in detail considering its hydrodynamics.[7,8] Rizvi et al. proposed another swimmer which was inspired by Najafi–Golestanian swimmer. They put three spheres on a triangular geometry configuration.[9] Avron et al. also proposed a simple swimmer consisting of two spherical bladders and a linear actuator. They called it pushme–pullyou swimmer.[10] Libersa et al. introduced a peculiar actuator which makes in-pipe microrobots crawling like an earthworm.[11] There are various kinds of low Reynolds swimmers, but these are the simple ones. Another microswimmer which can be an inspiration for designing new swimmers is Quadroar.[12] Quadroar is a swimmer with four rotational disks (oars) and a linear actuator. A swimmer having some similarties to our proposed robot was a three-disk swimmer that could move along its body axis in one dimension with just two linear actuators.[13]

Building and locomotion in small-scale is a challenging subject in science and technology. Some swimmers receive their energy from their environment by chemical reactions, like Paxton[14] and Sanchez swimmer.[15] These types of swimmers are very vulnerable and they need a specific condition for proper performance and building a swimmer that can tolerate a target environment like human blood is not an easy work. These problems could be solved by using magnetics fields. Magnetic field with low frequency does not have any serious side effect on the human body and it can permeate easily through it, therefore, it seems to be a good power source.[16] Electromagnetic micromotors are another option for the rotation. Li et al. designed an omnidirectional microrobot with an axial flux micromotor which works like common actuators.[17] Hamilton et al. designed and built a flagella-based swimmer and investigated its swimming ability experimentally.[18] Grosjean et al. also fabricated the Najafi–Golestanian swimmer and examined it on the air–water interface.[19]

Despite considerable progress in the field of microswimmers, most of the proposed swimmers have low degrees of freedom and their motion is restricted to a plane or limited maneuvers in space. In this study, we aim to address this issue by introducing a high maneuverable and controllable robot. For this purpose, we design a new swimmer with four actuators, then analyze its hydrodynamics and finally control its motion. As it was mentioned earlier, our swimmer is inspired by "Quadroar".[14] "Quadroar" is an I-shaped swimmer with a linear actuator on the middle link and four rotating disks on the legs. Despite the high maneuverability of "Quadroar", based on the dynamical equations governing the motion of this swimmer, it can be shown that the controllability matrix is not full rank and hence all of the coordinates of this swimmer cannot be controlled simultaneously. Consequently, we tried to design a new microswimmer with a higher rank of controllability matrix capable to perform more complex maneuvers in space. Our swimmer combines rotations of two disks and two telescopic motions of its body links and there is a sphere on the middle section of the swimmer body. The central sphere provides the space for the swimmer's accessories, such as the control unit, battery and sensors which are placed there. The two main features of the swimmer in maneuverability are: (i) it can rotate about all of its principal axes and reorients to the desired orientation and stroke along any desired 3D path with negligible side drift, (ii) it can be controlled to track prescribed 3D paths with continuous operation of the actuators based on a cascade control scheme.

In the following section, we introduce the geometry of the swimmer and derive its motion equations. In Section 3, we derive the dynamics of the swimmer and finally, the control scheme is discussed in Section 4.

2. Geometry and Kinematics

First of all, the swimmer will be introduced. The geometry of the swimmer that consists of two links, two similar disks of radius a and a sphere of radius r between two disks have been shown in Fig. 1. The length of the body link varies by the linear actuators, and disks can rotate continuously

https://doi.org/10.1017/S0263574720001289 Published online by Cambridge University Press

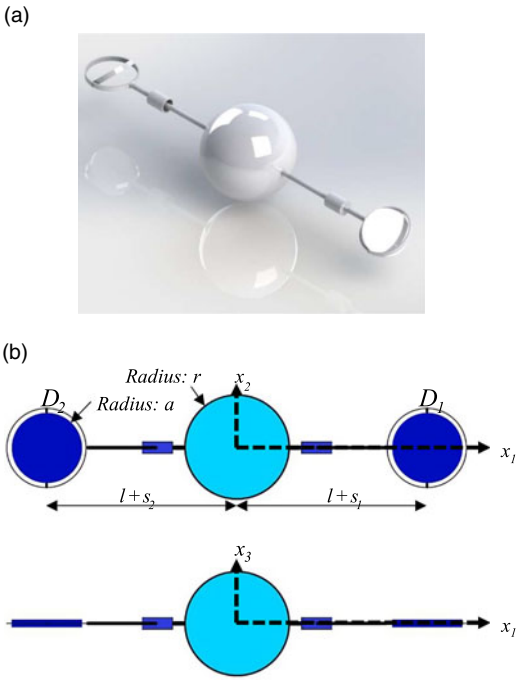


Fig. 1. The geometry of the swimmer. There are two linear actuators on the swimmer's body links. The park configuration is when disks are in $x_1 - x_2$ plane. The proposed swimmer has four degrees of freedom, two linear actuators and two rotational actuators on disks (β_n).

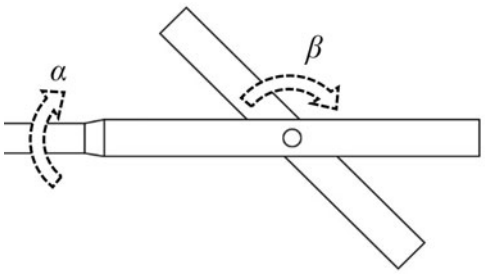


Fig. 2. One oar of the swimmer and its rotational angles (α_n, β_n).

or stepwise about the perpendicular axis of the body link. The length of the body links are $l + s_1$ and $l + s_2$, where s_n ($n = 1, 2$) is the expansion and contraction length of the linear actuators. The rotation of each disk about the robot body axes is measured by one angle β_n (see Fig. 2). It should be noted that the angle α_n is fixed and does not change with time.

The inertial coordinates are denoted by (X_1 X_2 X_3) and its corresponding basic vectors are ($\boldsymbol{E}_1$ $\boldsymbol{E}_2$ $\boldsymbol{E}_3$) respectively. The position of the swimmer mass center is defined as $\boldsymbol{X}_c = (X_{c1}\ X_{c2}\ X_{c3})$ describing the translational motion of the swimmer in the inertial coordinates. The swimmer orientation is determined by Euler angles, ($\phi\ \theta\ \psi$). We choose the order of axes transformation as $\psi \rightarrow \theta \rightarrow \phi$ with axes order of rotation as $3 \rightarrow 2 \rightarrow 1$. The defined angles ($\phi\ \theta\ \psi$) are roll, pitch and yaw angles, respectively. We also defined a body-fixed coordinate, (x_1 x_2 x_3), with the unit vector ($\boldsymbol{e}_1$ $\boldsymbol{e}_2$ $\boldsymbol{e}_3$), whose x_1 is along the body link and axes x_2 and x_3 are perpendicular to x_1 as shown in Fig. 1. Defining $\boldsymbol{R}_{x_i}(\gamma)$ as a rotation matrix about the x_i axis by the angle γ, transformation from $\boldsymbol{E}_i$ to $\boldsymbol{e}_i$ (i = 1,2,3) is carried out using the following equation:

$$\boldsymbol{e}_i = \boldsymbol{R}_{x_1}(\phi)\ .\ \boldsymbol{R}_{x_2}(\theta)\ .\ \boldsymbol{R}_{x_3}(\psi)\ .\ \boldsymbol{E}_i = \boldsymbol{R}\boldsymbol{E}_i,$$

https://doi.org/10.1017/S0263574720001289 Published online by Cambridge University Press

where $\boldsymbol{R}_{x_i}$ matrices are rotational matrices. The transformation matrices for roll–pitch–yaw rotations are defined as

$$\text{Roll: } R_{x_1}(\phi) = \begin{bmatrix} 1 & 0 & 0 \\ 0 & \cos\phi & \sin\phi \\ 0 & -\sin\phi & \cos\phi \end{bmatrix}$$

$$\text{Pitch: } R_{x_2}(\theta) = \begin{bmatrix} \cos\theta & 0 & -\sin\theta \\ 0 & 1 & 0 \\ \sin\theta & 0 & \cos\theta \end{bmatrix}$$

$$\text{Yaw:} R_{x_3}(\psi) = \begin{bmatrix} \cos\psi & \sin\psi & 0 \\ -\sin\psi & \cos\psi & 0 \\ 0 & 0 & 1 \end{bmatrix}$$

Using the angular velocity of the swimmer in the body frame denoted by $\boldsymbol{\Omega}$, the velocity of each oar (disk) can be obtained as follows:

$$\boldsymbol{v}_n = \boldsymbol{R}\boldsymbol{v}_c + \dot{l}_n\boldsymbol{e}_1 + \boldsymbol{\Omega}\times l_n\boldsymbol{e}_1, \tag{2}$$

where the over-dot denotes d/dt, $n = 1, 2$ and

$$l_1 = +(s_1 + l), \quad l_2 = -(s_2 + l), \tag{3}$$

The linear actuators expand when $\dot{s}_n > 0$ and contract when $\dot{s}_n < 0$. For the sake of compact notation, let $s(\gamma)$ and $c(\gamma)$ denote $\sin(\gamma)$ and $\cos(\gamma)$, respectively. The absolute angular velocities of the disks are

$$\boldsymbol{\omega}_n = \boldsymbol{\Omega} + \begin{bmatrix} \mathrm{c}(\alpha_n) & 0 & -\mathrm{s}(\alpha_n) \\ 0 & 1 & 0 \\ \mathrm{s}(\alpha_n) & 0 & \mathrm{c}(\alpha_n) \end{bmatrix} \begin{pmatrix} \dot{\beta}_n \\ 0 \\ 0 \end{pmatrix} \tag{4}$$

As it is mentioned earlier, $s_n(t)$, $\beta_n(t)$, where $n = 1, 2$, are the four control inputs of the swimmer and α_n $(n = 1, 2)$ is the angle of each disk about the longitudinal axis of swimmer which is fixed. The swimmer can move along and rotate about any of its body axes. In Section 3, we will show how the swimmer swims.

3. Swimming and Reorientation

We ignore the drag forces and torques on the body link because its effective cross-section area is negligible compared to disks and the sphere. The required force and torque for translation and rotation come from the interaction of disks and the fluid resistance as the disks rotate or move. We assumed that the fluid streams around the disks and the sphere do not affect each other. For this assumption, they should be far enough from each other, which means that $a, r \ll l$. For more accurate results, the hydrodynamic interactions between the disks and the sphere with each other should appear in the force and torque equations.[20]

The translation tensor of a circular disk which has no acceleration can be expressed as follows:[21]

$$\boldsymbol{K}_{disk} = \left(\frac{32}{3}\boldsymbol{i}_1\boldsymbol{i}_1 + \frac{32}{3}\boldsymbol{i}_2\boldsymbol{i}_2 + 16\boldsymbol{i}_3\boldsymbol{i}_3\right) a, \tag{5}$$

where $(\boldsymbol{i}_1\ \boldsymbol{i}_2\ \boldsymbol{i}_3)$ define an orthogonal coordinate system fixed to the disk. The origin of the coordinate system coincides with the disk's center of mass, where $\boldsymbol{i}_3$ is normal to the disk plane. The translation tensor of a sphere could be obtained from the following equation:

$$\boldsymbol{K}_{sphere} = 6\pi r\boldsymbol{I}, \tag{6}$$

https://doi.org/10.1017/S0263574720001289 Published online by Cambridge University Press

where r is the radius of the sphere and $\boldsymbol{I}$ is the identity matrix. For a surrounding fluid with dynamic viscosity of μ, the drag force experienced by a disk when moving with the velocity $\boldsymbol{v}_n$ is

$$\boldsymbol{F}_n = -\mu \boldsymbol{K}_{disk,n} \boldsymbol{v}_n \tag{7}$$

The relation between body and disks coordinate systems is

$$\begin{pmatrix} \boldsymbol{i}_1 \\ \boldsymbol{i}_2 \\ \boldsymbol{i}_3 \end{pmatrix} = \begin{bmatrix} 1 & 0 & 0 \\ 0 & \mathrm{c}(\beta_n) & \mathrm{s}(\beta_n) \\ 0 & -\mathrm{s}(\beta_n) & \mathrm{c}(\beta_n) \end{bmatrix} \begin{bmatrix} \mathrm{c}(\alpha_n) & 0 & -\mathrm{s}(\alpha_n) \\ 0 & 1 & 0 \\ \mathrm{s}(\alpha_n) & 0 & \mathrm{c}(\alpha_n) \end{bmatrix} \begin{pmatrix} \boldsymbol{e}_1 \\ \boldsymbol{e}_2 \\ \boldsymbol{e}_3 \end{pmatrix} \tag{8}$$

Therefore, the $\boldsymbol{K}$ matrix in body-fixed coordinates is obtained from

$$\boldsymbol{K}_{disk,n} = \frac{8}{3} a \begin{bmatrix} 4\left(\sin^2\alpha_n + \cos^2\beta_n\right) + 2\sin^2\alpha_n \cos^2\beta_n & -\sin 2\beta_n \sin\alpha_n & 2\sin\alpha_n \left(2\cos\alpha_n - 2\cos\beta_n + \cos\alpha_n \cos^2\beta_n\right) \\ -\sin 2\beta_n \sin\alpha_n & 4 + 2\cos^2\beta_n & -\sin 2\beta_n \cos\alpha_n \\ 2\sin\alpha_n \left(2\cos\alpha_n - 2\cos\beta_n + \cos\alpha_n \cos^2\beta_n\right) & -\sin 2\beta_n \cos\alpha_n & 4 + 2\cos^2\beta_n - 2\sin^2\alpha_n \cos^2\alpha_n \end{bmatrix} \tag{9}$$

The force on the sphere could be obtained from

$$\boldsymbol{F}_{sphere} = -\mu \boldsymbol{K}_{sphere} \boldsymbol{v}_c \tag{10}$$

The swimmer is designed to be neutrally buoyant and if we assume the acceleration of the swimmer is small, which is a reasonable assumption in low Reynolds regime, then the total drag forces must be zero and we have a force balance equation as follows:

$$\mu \left(\sum_{n=1}^{2} \boldsymbol{K}_{disk,n} \boldsymbol{v}_n + \boldsymbol{K}_{sphere} \boldsymbol{v}_c \right) = 0 \tag{11}$$

The resistive torque that a circular disk and a sphere experience due to their pure rotation can be expressed as follows:[21]

$$\boldsymbol{\tau}_{disk,n} = -\mu \boldsymbol{G}_{disk,n} \boldsymbol{\omega}_n, \quad \boldsymbol{G}_{disk,n} = \frac{32}{3} a^3 \boldsymbol{I} \tag{12}$$

$$\boldsymbol{\tau}_{sphere} = -\mu \boldsymbol{G}_{sphere} \boldsymbol{\Omega}, \quad \boldsymbol{G}_{sphere} = 8\pi r^3 \boldsymbol{I}(13), \tag{13}$$

where $\boldsymbol{I}$ is the identity matrix and $\boldsymbol{G}$ is the rotation tensor. The resultant torque exerted on the swimmer about its center of mass is the sum of $\boldsymbol{\tau}$ and the moments $\boldsymbol{l}_n \times \boldsymbol{F}_n$ which are torques that the drag forces generate about the center of mass of the swimmer. Consequently, the torque balance equation becomes

$$\mu \sum_{n=1}^{2} \left[\boldsymbol{G}_{disk,n} \boldsymbol{\omega}_n + \boldsymbol{l}_n \times \left(\boldsymbol{K}_{disk,n} \boldsymbol{v}_n \right) \right] + \mu \boldsymbol{G}_{sphere} \boldsymbol{\Omega} = 0 \tag{14}$$

By substituting Eqs. (2) and (4) in force and torque balance equations, we obtain

$$\begin{bmatrix} \boldsymbol{C}_{11} & \boldsymbol{C}_{12} \\ \boldsymbol{C}_{21} & \boldsymbol{C}_{22} \end{bmatrix} \begin{pmatrix} \boldsymbol{v}_c \\ \boldsymbol{\Omega} \end{pmatrix} = \begin{pmatrix} f_1 \\ f_2 \end{pmatrix} \tag{15}$$

Due to the ignorance of inertial forces, the equation is linear respect to $\boldsymbol{v}_c$ and $\boldsymbol{\Omega}$. By solving Eq. (15), the velocities are determined and the position can be found by direct integration. To find the swimmer orientation, kinematic equations relating the rate of Euler angles to angular velocity will be used. Now after derivation of the governing equations of motion, a controller will be designed for the proposed swimmer.

To further clarify the swimming behavior of the proposed microrobot, some simple motion modes are investigated. For this purpose, at first the rotational actuators are fixed and the prismatic ones are actuated with a ramp function. To conduct the simulation, the system parameters are set as $a = 1\ \mu\mathrm{m}$,

https://doi.org/10.1017/S0263574720001289 Published online by Cambridge University Press

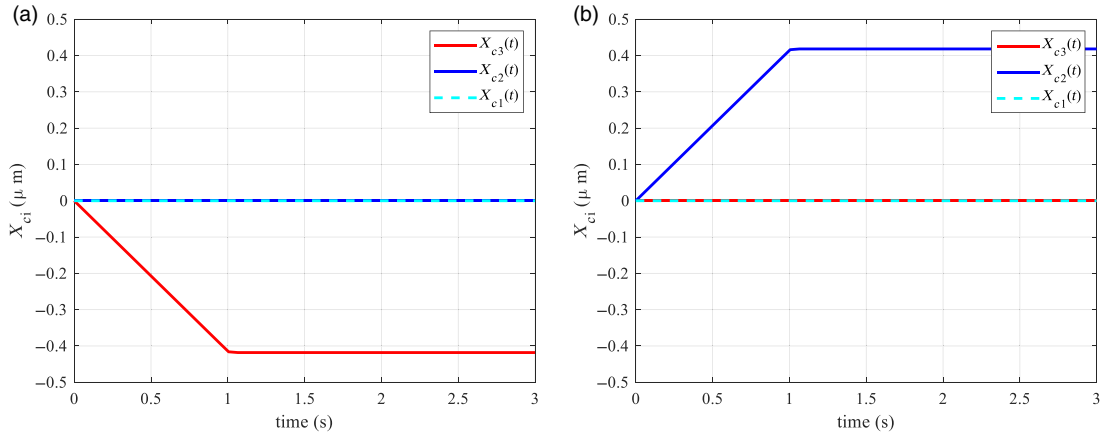


Fig. 3. Simple translational motion modes of the microswimmer. Results are obtained for fixed disks angles and ramp function expansion of the linear actuators. (a) $\alpha_1, \alpha_2 = 0$ (b) $\alpha_1, \alpha_2 = \pi/2$.

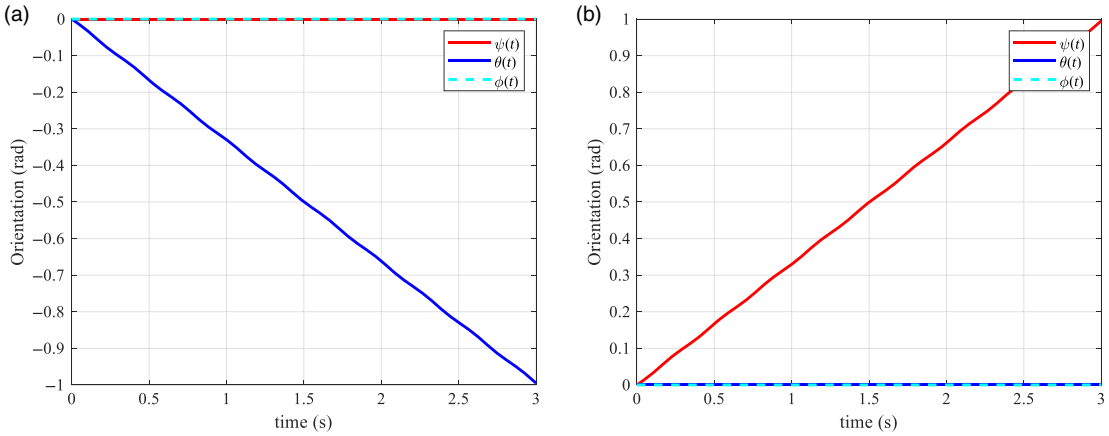


Fig. 4. Simple rotational motion modes of the microswimmer. Results are obtained when the linear actuators are fixed and rotational ones rotate with constant speed (10 rad/s) while the angles α_1 and α_2 are set as (a) zero (b) $\pi/2$.

$l = 40$ μm and $r = 2$ μm. The disks have been fixed with the following angles:

$$\alpha_1 = 0, \alpha_2 = 0$$
$$\beta_1 = \pi/4, \beta_2 = -\pi/4$$

The prismatic actuators are excited with the ramp function as follows:

$$s_1 = s_2 = \begin{cases} 5t, & t \leq 1 \\ 5, & t > 1 \end{cases}, (\mu\text{m})$$

If the prismatic actuators expand according to the mentioned function, it is expected that a force is generated along the axis x_3 on the swimmer. This force moves the swimmer along x_3 (see Fig. 3(a)). If we set the angles α_1 and α_2 to $\pi/2$ instead of zero, while the angles β_1 and β_2 are the same as before, in the case of expansion of the prismatic actuators, the swimmer moves along the axis x_2 (see Fig. 3(b)).

For analyzing the effect of rotational actuators on the swimmer, another simulation has been run. The linear actuators are fixed and the angles α_1 and α_2 are set as zero. The disk angles β_1 and β_2 are changed with a constant speed (10 rad/s). As it is expected, the swimmer just rotates around the axis x_2. The results are shown in Fig. 4(a). If all actuations are the same as before, except the angles α_1 and α_2 which are set to $\pi/2$ instead of zero, the microswimmer rotates around its x_3 axis. (see Fig. 4(b)).

https://doi.org/10.1017/S0263574720001289 Published online by Cambridge University Press

4. Controlling Method

In this section, we rewrite the equations of motion in a form suitable for the design of the controller. To this aim, if we consider six equations of motion appeared in relation (15) and separate the actuators efforts $\dot{s}_1$, $\dot{s}_2$, $\dot{\beta}_1$ and $\dot{\beta}_2$ from therate of state variables, then the following equation can be obtained:

$$\boldsymbol{A}_{6\times6}\begin{pmatrix}\dot{X}_{c_1}\\ \dot{X}_{c_2}\\ \dot{X}_{c_3}\\ \dot{\phi}\\ \dot{\theta}\\ \dot{\psi}\end{pmatrix}+\boldsymbol{B}_{6\times4}\begin{pmatrix}\dot{s}_1\\ \dot{s}_2\\ \dot{\beta}_1\\ \dot{\beta}_2\end{pmatrix}=0 \tag{16}$$

Here, matrices $\boldsymbol{A}$ and $\boldsymbol{B}$ are in terms of swimmer position and orientation variables X_{c_1}, X_{c_2}, X_{c_3}, ϕ, θ and ψ. Since some of these matrices components are very complicated terms versus the swimmer state variables, they are not shown here (for more details see Appendix A). However, it should be noted that in the above equation, $\dot{\varphi}$ only appears in the fourth equation and it puts the matrix in bad condition. If we put away the fourth equation from others in Eq. (16), the following equation will be achieved:

$$\boldsymbol{A}_{\boldsymbol{15}\times5}\begin{pmatrix}\dot{X}_{c_1}\\ \dot{X}_{c_2}\\ \dot{X}_{c_3}\\ \dot{\theta}\\ \dot{\psi}\end{pmatrix}+\boldsymbol{B}_{\boldsymbol{15}\times4}\begin{pmatrix}\dot{s}_1\\ \dot{s}_2\\ \dot{\beta}_1\\ \dot{\beta}_2\end{pmatrix}=0 \tag{17}$$

Here $\boldsymbol{A_1}$ and $\boldsymbol{B_1}$ are obtained using $\boldsymbol{A}$ and $\boldsymbol{B}$. Now, since our aim is to control the robot position to track any desired spatial trajectory, we can omit $\dot{\theta}$ and $\dot{\psi}$ from Eq. (17) and leave only position variables in this equation. To this aim, if we solve $\dot{\theta}$ and $\dot{\psi}$ from the first two equations and substitute the results in Eq. (17), then the following equation will be achieved:

$$\overline{\boldsymbol{A}}_{3\times3}\begin{pmatrix}\dot{X}_{c_1}\\ \dot{X}_{c_2}\\ \dot{X}_{c_3}\end{pmatrix}+\overline{\boldsymbol{B}}_{3\times4}\begin{pmatrix}\dot{s}_1\\ \dot{s}_2\\ \dot{\beta}_1\\ \dot{\beta}_2\end{pmatrix}=0 \tag{18}$$

Here, matrices $\overline{\boldsymbol{A}}$ and $\overline{\boldsymbol{B}}$ can be obtained using some mathematical operations on components of matrices $\boldsymbol{A_1}$ and $\boldsymbol{B_1}$. If we display Eq. (18) in the state-space form, then we have $\dot{\boldsymbol{X}}=\boldsymbol{A}'\boldsymbol{X}+\boldsymbol{B}'\boldsymbol{u}$, where $\boldsymbol{X}=\begin{bmatrix}X_{c_1} & X_{c_2} & X_{c_2}\end{bmatrix}^T$, $\boldsymbol{A}'_{3\times3}=[\boldsymbol{0}]_{3\times3}$, $\boldsymbol{u}=\begin{bmatrix}\dot{s}_1 & \dot{s}_2 & \dot{\beta}_1 & \dot{\beta}_2\end{bmatrix}^T$ and $\boldsymbol{B}'_{3\times4}=\overline{\boldsymbol{A}}^{-1}\overline{\boldsymbol{B}}$. All rows of matrix $\boldsymbol{B}'$ are strongly independent so the rank of $\boldsymbol{B}'$ is three. Now, we can calculate the rank of controllability matrix $[\boldsymbol{B}', \boldsymbol{A}'\boldsymbol{B}', \boldsymbol{A}'^{\boldsymbol{2}}\boldsymbol{B}']$, which will be three. Therefore the microswimmer can track any desired time trajectory in space by adjusting control inputs $\dot{s}_1$, $\dot{s}_2$, $\dot{\beta}_1$ and $\dot{\beta}_2$. On the other hand, since three outputs X_{c_1}, X_{c_2}, X_{c_3} must track desired time trajectories in space, the four control inputs introduce a degree of freedom which can be employed to optimize a desired cost function.

To this aim, we will use a cascade control strategy. The control system has two main loops. In the outercontrol loop, based on the desired trajectory, the robot velocity vector is calculated using a feed-forward plus a proportional controller as follows:

$$\begin{pmatrix}\dot{X}_{c_1}\\ \dot{X}_{c_2}\\ \dot{X}_{c_3}\end{pmatrix}=\begin{pmatrix}\dot{X}_{c_1}d\\ \dot{X}_{c_2}d\\ \dot{X}_{c_3}d\end{pmatrix}-k_p\begin{pmatrix}X_{c_1}-X_{c_{1d}}\\ X_{c_2}-X_{c_{2d}}\\ X_{c_3}-X_{c_{3d}}\end{pmatrix} \tag{19}$$

https://doi.org/10.1017/S0263574720001289 Published online by Cambridge University Press

Table I. Desired output and initial conditions of the swimmer.

$X_{c_{1d}}(t)$		$\begin{cases} 2.5t, & t \le 2 \\ 5, & t > 2 \end{cases}$, (μm)
$X_{c_{2d}}(t)$		$3\sin(2\pi/5t + \pi/3)$, (μm)
$X_{c_{3d}}(t)$		$4\sin(\pi/3t)$, (μm)
Initial condition	Location	[5 −2 −5] (μm)
	Orientation	[0 0 0]
Proportional controller coefficient (k_p)		4
σ		0.1

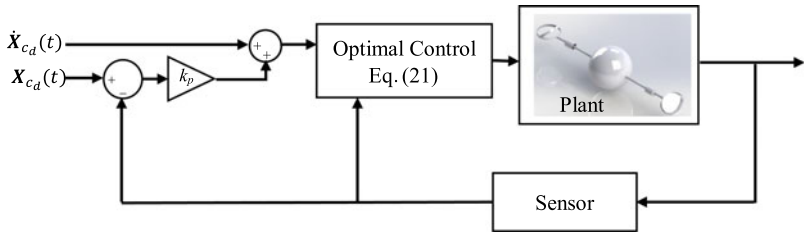


Fig. 5. Schematic of the designed control block diagram.

Substituting Eq. (19) into Eq. (18) results in:

$$\overline{A}_{3\times3}\left(\begin{pmatrix}\dot{X}_{c_1}d\\ \dot{X}_{c_2}d\\ \dot{X}_{c_3}d\end{pmatrix} - k_p\begin{pmatrix}X_{c_1}-X_{c_{1d}}\\ X_{c_2}-X_{c_{2d}}\\ X_{c_3}-X_{c_{3d}}\end{pmatrix}\right) + \overline{B}_{3\times4}\begin{pmatrix}\dot{s}_1\\ \dot{s}_2\\ \dot{\beta}_1\\ \dot{\beta}_2\end{pmatrix} = 0 \tag{20}$$

In the inner control loop, using an optimal control strategy, the actuation signals are computed in a way to ensure robot trajectory tracking with a minimum variation of control signals. To reduce the control signals fluctuations, a continuous-time cost function is defined as $\frac{1}{2}\left(\dot{s}_1{}^2 + \dot{s}_2{}^2\right) + \frac{\sigma}{2}(\dot{\beta}_1{}^2 + \dot{\beta}_2{}^2)$. Here, σ is a positive constant that is used to adjust the relative importance of the rotational terms with respect to linear terms in the cost function. Minimizing this cost function reduces the rate of change of actuation signals leading to more smooth control efforts. To this aim, considering the Eq. (20) as constraints, the following function must be minimized:

$$J = \frac{1}{2}\left(\dot{s}_1{}^2 + \dot{s}_2{}^2\right) + \frac{\sigma}{2}(\dot{\beta}_1{}^2 + \dot{\beta}_2{}^2) + \sum\nolimits_{i=1}^{3} \lambda_i \, eq_i \tag{21}$$

$$\frac{\partial J}{\partial \dot{s}_1} = 0, \quad \frac{\partial J}{\partial \dot{s}_2} = 0, \quad \frac{\partial J}{\partial \dot{\beta}_1} = 0, \quad \frac{\partial J}{\partial \dot{\beta}_2} = 0, \quad \frac{\partial J}{\partial \lambda_i} = 0 \; (i = 1, 2, 3) \tag{22}$$

Here, λ_i $(i = 1, 2, 3)$ are Lagrange multipliers. By solving Eq. (22), the inputs could be obtained. Despite the number of actuators in the proposed microswimmer is one less than Quadroar, the rank of controllability matrix in our robotis one more than Quadroar and this is the main advantage of our designed robot. The block diagram of the designed control strategy is shown in Fig. 5. In the real environment, the microswimmer may experience a variety sources of disturbances. A simple way to compensate the undesired effects of external disturbances is to add an integral term to the designed controller and change it from P to PI controller.

To demonstrate the performance of the designed cascade optimal control, we conducted a simulation. The angles α_n are fixed values which are set as $\alpha_1 = \pi/4, \; \alpha_2 = -\pi/4$ in our simulation. Table I lists the desired trajectory, the initial position, orientation, the proportional gain of the trajectory control and parameter σ. Figure 6 depicts how the robot position coordinates converge to their desired values.

According to the governing equations of motion of the microswimmer, the resultant force and torque on the robot must be zero. If we calculate the ratio of the resultant force to the force on central

https://doi.org/10.1017/S0263574720001289 Published online by Cambridge University Press

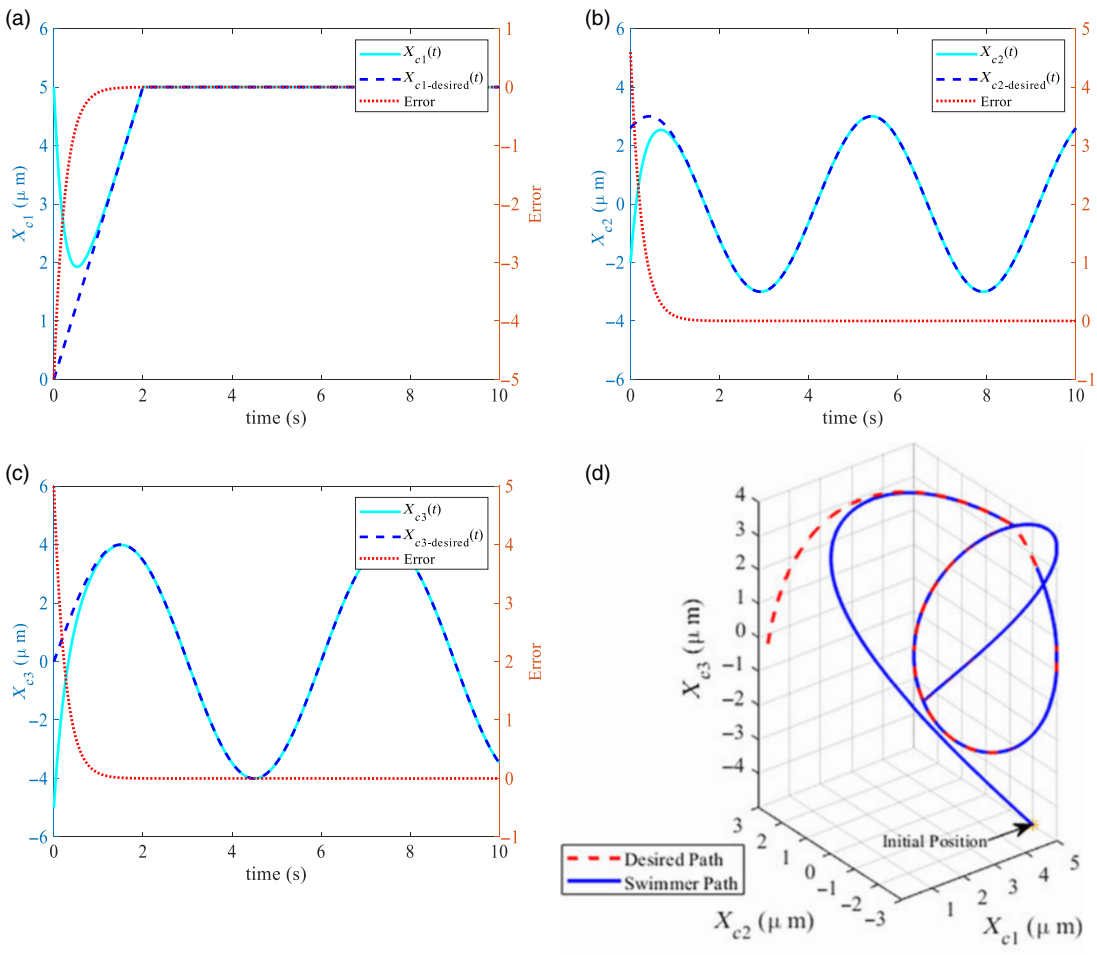


Fig. 6. Performance of the cascade control strategy proposed for trajectory tracking of the swimmer.

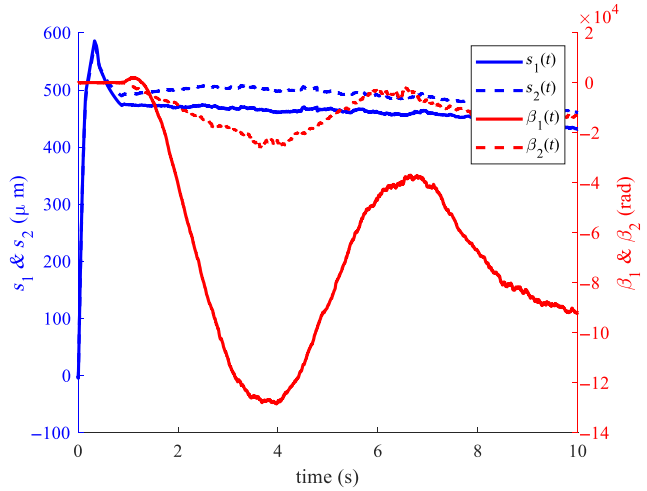


Fig. 7. Inputs required for the actuators to control the robot to track agiven reference trajectory.

sphere, the dimensionless error of force can be computed. Also, this can be repeated for calculation of the dimensionless error of torque. According to our calculations, these errors are in the order of10^{-11} which verifies the correctness of the model implemented in software.

As is indicated in Fig. 6, the robot perfectly follows the desired sinusoidal and ramp trajectories in 3D space. The required inputs for following the desired trajectory is shown in Fig. 7.

https://doi.org/10.1017/S0263574720001289 Published online by Cambridge University Press

The required actuation torques can be generated by electromagnetic motors. These actuators are installed on the swimmer and they are designed or selected depending on the required torques which can be calculated based on the microswimmer maneuverability expectations. If we assume that the microrobot swims in water, according to our selected trajectory, the required actuators torques are in the order of 10^{-20} N.m.

5. Discussions

The swimmer with two disks, a sphere and thin frictionless links provides a simple swimmer. The continuous operations of the actuators could lead to complex yet well-defined orbits, which are sensitive to the stroke length of the body links and its frequency. By analyzing the dynamics equations and controllability matrix, it was demonstrated that our swimmer is a good option for accurate swimming in low Reynolds number regimes. This maneuverability makes the swimmer suitable for noncontact fluidic manipulation of particles.[22] We introduced and applied a cascade control strategy, having two main control loops: a trajectory controller and an optimal controller. The trajectory controller is a proportional controller with a feed-forward term and the optimal controller minimizes the controller effort fluctuations. The controller has been simulated on the microswimmer and the results demonstrated its performance. We ignored physical limitations of the swimmer and its actuators. Putting some restrictions and developing the new controlling methods for some particular applications are interesting problems for future work. Mirzakhanloo et al. have studied on the Quadroar in a swarm and analyzed the dynamics of the swimmer with hydrodynamic interactions[23] and Daddi-Moussa-Ider et al. have simulated the three-sphere swimmer near a wall and studied its behavior.[24] Research on the hydrodynamic interactions between two swimmer and other objects in the fluids is an intriguing subject for the future study. The swimmer could be exploited in medical cases such as healing vein wall, so another goal for future could be an analysis of the swimmer hydrodynamics in circular channels. Demir and Yesilyurt did the same study for helical structures.[25]

Several groups in the micro/nanorobotics field are designing and building machines in micro to molecular scales, therefore our swimmer seems to be a realizable swimmer in the new future. They also did researches in chemistry and designed molecular motors that get their power from electrochemical,[14,26] photochemical[27] or magnetical[28,29] sources. With the large variety of actuators and manufacturing procedures in nano and micro-scale, our swimmer can be built and tested in the real world. Moreover, in the dynamic modeling of the swimmer, it has been assumed that the swimmer locomotion occurs at low-Reynolds-number flow. Hence, instead of micro-/nano-scale swimmer, it can be a milli-scale robot in a more viscous fluid such as silicon oil. A fluid with more viscosity is not violating the low Reynolds condition. A milli-scale swimmer could be fabricated with conventional methods.

6. Conclusion

In this study, a low-Reynolds-number swimmer has been proposed, a swimmer with four control inputs. It has two linear actuators and two disks which have one degree of freedom.One of the big advantages of the proposed swimmer is its ability to follow arbitrary trajectories in 3D space due to the high rank of the controllability matrix. A cascade control strategy was proposed where the outer controller loop guarantees the trajectory control based on a proportional controller with a feed-forward velocity term to track arbitrary trajectories and the inner control loop minimizes the fluctuations in the control efforts. The simulation results confirm the good performance of the closed-loop system.

Acknowledgment

The authors would like to thank the Iranian National Science Foundation (INSF) for their financial support.

References

1. D. Mahdy, R. Reda, N. Hamdi and I. S. Khalil, "Ultrasound-guided minimally invasive grinding for clearing blood clots: Promises and challenges," *IEEE Instrum. Meas. Mag.* **21**(2), 10–14 (2018).
2. M. Medina-Saìnchez, L. Schwarz, A. K. Meyer, F. Hebenstreit and O. G. Schmidt, "Cellular cargo delivery: Toward assisted fertilization by sperm-carrying micromotors," *Nano Lett.* **16**(1), 555–561 (2015).
3. B. J. Nelson, I. K. Kaliakatsos and J. J. Abbott, "Microrobots for minimally invasive medicine," *Ann. Rev. Biomed. Eng.* **12**(1), 55–85 (2010).

https://doi.org/10.1017/S0263574720001289 Published online by Cambridge University Press

4. E. M. Purcell, "Life at low Reynolds number," *Am. J. Phys.* **45**(1), 3–11 (1977).
5. E. Lauga and T. R. Powers, "The hydrodynamics of swimming microorganisms," *Rep. Prog. Phys.* **72**(9), 096601 (2009).
6. A. Najafi and R. Golestanian, "Simple swimmer at low Reynolds number: Three linked spheres," *Phys. Rev. E* **69**(6), 062901 (2004).
7. R. Golestanian and A. Ajdari, "Analytic results for the three-sphere swimmer at low Reynolds number," *Phys. Rev. E* **77**(3), 036308 (2008).
8. G. Alexander, C. Pooley and J. Yeomans, "Hydrodynamics of linked sphere model swimmers," *J. Phys. Condens. Matter* **21**(20), 204108 (2009).
9. M. S. Rizvi, A. Farutin and C. Misbah, "Three-bead steering microswimmers," *Phys. Rev. E 97*(2), 023102 (2018).
10. J. Avron, O. Kenneth and D. Oaknin, "Pushmepullyou: An efficient micro-swimmer," *New J. Phys.* **7**(1), 234 (2005).
11. C. Libersa, M. Arsicault, J.-P. Gazeau and J.-P. Lallemand, "A peculiar flip-flop actuator for an in-pipe microrobot," *Robotica* **22**(5), 547–561 (2004).
12. M. A. Jalali, M.-R. Alam and S. Mousavi, "Versatile low-Reynolds-number swimmer with three-dimensional maneuverability," *Phys. Rev. E* **90**(5), 053006 (2014).
13. Y. Ota, Y. Hosaka, K. Yasuda and S. Komura, "Three-disk microswimmer in a supported fluid membrane," *Phys. Rev. E* **97**(5), 052612 (2018).
14. W. F. Paxton, K. C. Kistler, C. C. Olmeda, A. Sen, S. K. St. Angelo, Y. Cao, T. E. Mallouk, P. E. Lammert and V. H. Crespi, "Catalytic nanomotors: Autonomous movement of striped nanorods," *J. Am. Chem. Soc.* **126**(41), 13424–13431 (2004).
15. S. Sanchez, A. A. Solovev, S. Schulze and O. G. Schmidt, "Controlled manipulation of multiple cells using catalytic microbots," *Chem. Commun.* **47**(2), 698–700 (2011).
16. K. E. Peyer, L. Zhang and B. J. Nelson, "Bio-inspired magnetic swimming microrobots for biomedical applications," *Nanoscale* **5**(4), 1259–1272 (2013).
17. Z. Li, J. Chen and J. Feng, "Design of an omni-directional mobile microrobot (OMMR-I) for a micro-factory with 2 mm electromagnetic micromotors," *Robotica* **23**(1), 45–49 (2005).
18. J. K. Hamilton, A. D. Gilbert, P. G. Petrov and F. Y. Ogrin, "Torque driven ferromagnetic swimmers," *Phys. Fluids* **30**(9), 092001 (2018).
19. G. Grosjean, M. Hubert, G. Lagubeau and N. Vandewalle, "Realization of the Najafi-Golestanian microswimmer," *Phys. Rev. E* **94**(2), 021101 (2016).
20. M. A. Jalali, A. Khoshnood and M.-R. Alam, "Microswimmer-induced chaotic mixing," *J. Fluid Mech.* **779**(18), 669–683 (2015).
21. J. Happel and H. Brenner, *Low Reynolds Number Hydrodynamics: With Special Applications to Particulate Media* (Springer Netherlands, 2012).
22. S. Floyd, C. Pawashe and M. Sitti, "Two-dimensional contact and noncontact micromanipulation in liquid using an untethered mobile magnetic microrobot," *IEEE Trans. Robot.* **25**(6), 1332–1342 (2009).
23. M. Mirzakhanloo, M. A. Jalali and M.-R. Alam, "Hydrodynamic choreographies of microswimmers," *Sci. Rep.* **8**(1), 3670 (2018).
24. A. Daddi-Moussa-Ider, M. Lisicki, C. Hoell and H. Löwen, "Swimming trajectories of a three-sphere microswimmer near a wall," *J. Chem. Phys.* **148**(13), 134904 (2018).
25. E. Demir and S. Yesilyurt, "Low Reynolds number swimming of helical structures in circular channels," *J. Fluids Struct.* **74**(7), 234–246 (2017).
26. J. Gibbs and Y. Zhao, "Catalytic nanomotors: Fabrication, mechanism, and applications," *Front. Mater. Sci.* **5**(1), 25–39 (2011).
27. N. Metzger, M. Mazilu, L. Kelemen, P. Ormos and K. Dholakia, "Observation and simulation of an optically driven micromotor," *J. Opt.* **13**(4), 044018 (2011).
28. P. Fischer and A. Ghosh, "Magnetically actuated propulsion at low Reynolds numbers: Towards nanoscale control," *Nanoscale* **3**(2), 557–563 (2011).
29. S. Tottori, L. Zhang, F. Qiu, K. K. Krawczyk, A. Franco-Obregón and B. J. Nelson, "Magnetic helical micromachines: Fabrication, controlled swimming, and cargo transport," *Adv. Mater.* **24**(6), 811–816 (2012).

Appendix A

Here Eq. (16) is going to be explained with more details. The $\boldsymbol{A}$ matrix in Eq. (16) is like the following:

$$\boldsymbol{A} = \begin{bmatrix} A_{11} & A_{12} & A_{13} & 0 & A_{15} & A_{16} \\ A_{21} & A_{22} & A_{23} & 0 & A_{25} & A_{26} \\ A_{31} & A_{32} & A_{33} & 0 & A_{35} & A_{36} \\ 0 & 0 & 0 & A_{44} & 0 & A_{46} \\ A_{51} & A_{52} & A_{53} & 0 & A_{55} & A_{56} \\ A_{61} & A_{62} & A_{63} & 0 & A_{65} & A_{66} \end{bmatrix} \tag{A1}$$

https://doi.org/10.1017/S0263574720001289 Published online by Cambridge University Press

Where A_{ii} are the matrix components in terms of physical dimensions and current configuration of the swimmer. Since all A_{i4} elements except A_{44} are zero, $\dot{\varphi}$ only appears in the fourth equation and if we put away the fourth equation from others in Eq. (16), the Eq. (17) will be achieved. $\boldsymbol{A_1}$ matrix is $\boldsymbol{A}$ matrix without fourth row and fourth column. The $\boldsymbol{B}$ matrix in Eq. (16) is represented in Eq. (A2).

$$\boldsymbol{B} = \begin{bmatrix} B_{11} & B_{12} & 0 & 0 \\ B_{21} & B_{22} & 0 & 0 \\ B_{31} & B_{32} & 0 & 0 \\ 0 & 0 & 0 & 0 \\ B_{51} & B_{52} & B_{53} & B_{54} \\ B_{61} & B_{62} & B_{63} & B_{64} \end{bmatrix} \tag{A2}$$

$\boldsymbol{B_1}$ matrix is $\boldsymbol{B}$ matrix without fourth row. The first two rows in Eq. (17) could be written as following:

$$\begin{bmatrix} A_{15} & A_{16} \\ A_{25} & A_{26} \end{bmatrix} \begin{pmatrix} \dot{\theta} \\ \dot{\psi} \end{pmatrix} + \begin{bmatrix} A_{11} & A_{12} & A_{13} \\ A_{21} & A_{22} & A_{23} \end{bmatrix} \begin{pmatrix} \dot{X}_{c_1} \\ \dot{X}_{c_2} \\ \dot{X}_{c_3} \end{pmatrix} + \boldsymbol{B'}_{\mathbf{1}2\times 4} \begin{pmatrix} \dot{s}_1 \\ \dot{s}_2 \\ \dot{\beta}_1 \\ \dot{\beta}_2 \end{pmatrix} = 0 \tag{A3}$$

Where A_{ii} are components of matrix $\boldsymbol{A}$ and $\boldsymbol{B'_1}$ is first two rows of $\boldsymbol{B_1}$. By solving Eq. (A3) for $\dot{\theta}$ and $\dot{\psi}$, these two variables could be derived in terms of other variables including $\dot{X}_{c_1}$, $\dot{X}_{c_2}$, $\dot{X}_{c_3}$, $\dot{s}_1$, $\dot{s}_2$, $\dot{\beta}_1$, and $\dot{\beta}_2$. If the derived results are substituted in Eq. (17) and simplified, the Eq. (18) will be achieved.

The $\overline{\boldsymbol{B}}$ matrix in Eq. (18) can be presented as follows:

$$\overline{\boldsymbol{B}} = \begin{bmatrix} \overline{B}_{11} & \overline{B}_{12} & 0 & 0 \\ \overline{B}_{21} & \overline{B}_{22} & \overline{B}_{23} & \overline{B}_{24} \\ \overline{B}_{31} & \overline{B}_{32} & \overline{B}_{33} & \overline{B}_{34} \end{bmatrix} \tag{A4}$$

All rows of matrix $\overline{\boldsymbol{B}}$ are strongly independent so the rank of $\overline{\boldsymbol{B}}$ is three.

Components of matrices $\boldsymbol{A}$ and $\boldsymbol{B}$ are displayed as follows:

$$\begin{aligned}
A_{11} = {} & (16\,a\,\cos(\psi)\cos(\theta)\,(\sin^2(\beta_1)+2))/3 + (16\,a\,\cos(\psi)\,\cos(\theta)\,(\sin^2(\beta_2)+2))/3 \\
& + 6\,\pi r\,\cos(\psi)\,\cos(\theta) + (16\,a\,\cos(\alpha_1)\,\cos(\beta_1)\,\sin(\beta_1)\,(\sin(\phi)\,\sin(\psi) \\
& + \cos(\phi)\,\cos(\psi)\,\sin(\theta)))/3 + (16\,a\,\cos(\alpha_2)\,\cos(\beta_2)\,\sin(\beta_2)\,(\sin(\phi)\,\sin(\psi) \\
& + \cos(\phi)\,\cos(\psi)\,\sin(\theta)))/3 + (16\,a\,\cos(\beta_1)\,\sin(\alpha_1)\,\sin(\beta_1)\,(\cos(\phi)\,\sin(\psi) \\
& - \cos(\psi)\,\sin(\phi)\,\sin(\theta)))/3 + (16\,a\,\cos(\beta_2)\,\sin(\alpha_2)\,\sin(\beta_2)\,(\cos(\phi)\,\sin(\psi) \\
& - \cos(\psi)\,\sin(\phi)\,\sin(\theta)))/3 \\
A_{12} = {} & (16\,a\,\cos(\theta)\,\sin(\psi)\,(\sin^2(\beta_1)+2))/3 + (16\,a\,\cos(\theta)\,\sin(\psi)\,(\sin^2(\beta_2)+2))/3 \\
& + 6\,\pi r\,\cos(\theta)\,\sin(\psi) - (16\,a\,\cos(\alpha_1)\,\cos(\beta_1)\,\sin(\beta_1)\,(\cos(\psi)\,\sin(\phi) \\
& - \cos(\phi)\,\sin(\psi)\,\sin(\theta)))/3 - (16\,a\,\cos(\alpha_2)\,\cos(\beta_2)\,\sin(\beta_2)\,(\cos(\psi)\,\sin(\phi) \\
& - cos(\phi)\,\sin(\psi)\,\sin(\theta)))/3 - (16\,a\,\cos(\beta_1)\,\sin(\alpha_1)\,\sin(\beta_1)\,(\cos(\phi)\,\cos(\psi) \\
& + \sin(\phi)\,\sin(\psi)\,\sin(\theta)))/3 - (16\,a\,\cos(\beta_2)\,\sin(\alpha_2)\,\sin(\beta_2)\,(\cos(\phi)\,\cos(\psi) \\
& + \sin(\phi)\,\sin(\psi)\,\sin(\theta)))/3 \\
A_{13} = {} & (16\,a\,\cos(\phi)\,\cos(\theta)\,\cos(\alpha_1)\,\cos(\beta_1)\,\sin(\beta_1))/3 - (16\,a\,\sin(\theta)\,(\sin(\beta_2)\hat{}2+2))/3 \\
& - 6\,\pi r\,\sin(\theta) - (16\,a\,\sin(\theta)\,(\sin(\beta_1)\hat{}2+2))/3 \\
& + (16\,a\,\cos(\phi)\,\cos(\theta)\,\cos(\alpha_2)\,\cos(\beta_2)\,\sin(\beta_2))/3 \\
& - (16\,a\,\cos(\theta)\,\cos(\beta_1)\,\sin(\phi)\,\sin(\alpha_1)\,\sin(\beta_1))/3 \\
& - (16\,a\,\cos(\theta)\,\cos(\beta_2)\,\sin(\phi)\,\sin(\alpha_2)\,\sin(\beta_2))/3
\end{aligned}$$

https://doi.org/10.1017/S0263574720001289 Published online by Cambridge University Press

$$A_{14} = 0$$

$$\begin{aligned}A_{15} = {} & (16\,a\,cos(\phi)\,cos(\alpha_2)\,cos(\beta_2)\,sin(\beta_2)\,(l+s_2))/3 \\ & -(16\,a\,cos(\phi)\,cos(\alpha_1)\,cos(\beta_1)\,sin(\beta_1)\,(l+s_1))/3 \\ & +\,(16\,a\,sin(\phi)\,cos(v12)\,sin(\alpha_1)\,sin(\beta_1)\,(l+s_1))/3 \\ & -(16\,a\,sin(\phi)\,cos(\beta_2)\,sin(\alpha_2)\,sin(\beta_2)\,(l+s_2))/3\end{aligned}$$

$$\begin{aligned}A_{16} = {} & (16\,a\,cos(\phi)\,cos(\theta)\,cos(\beta_2)\,sin(\alpha_2)\,sin(\beta_2)\,(l+s_2))/3 \\ & -(16\,a\,cos(\theta)\,sin(\phi)\,cos(\alpha_1)\,c\phi\phi s(\beta_1)\,sin(\beta_1)\,(l+s_1))/3 \\ & -(16\,a\,cos(\phi)\,cos(\theta)\,cos(\beta_1)\,sin(\alpha_1)\,sin(\beta_1)\,(l+s_1))/3 \\ & +\,(16\,a\,cos(\theta)\,sin(\phi)\,cos(\alpha_2)\,cos(\beta_2)\,sin(\beta_2)\,(l+s_2))/3\end{aligned}$$

$$\begin{aligned}A_{21} = {} & -6\,\pi r\,(cos(\phi)\,sin(\psi) - cos(\psi)\,sin(\phi)\,sin(\theta)) - (16\,a\,(cos(\phi)\,sin(\psi) \\ & -cos(\psi)\,sin(\phi)\,sin(\theta))\,(-\sin^2(\alpha_1)\,\sin^2(\beta_1) + \sin^2(\alpha_1) + 2))/3 \\ & -(16\,a\,(cos(\phi)\,sin(\psi) - cos(\psi)\,sin(\phi)\,sin(\theta))\,(-sin(\alpha_2)\hat{}2\,sin(\beta_2)\hat{}2 \\ & +\,sin(\alpha_2)\hat{}2 + 2))/3 - (16\,a\,cos(\alpha_1)\,cos(\beta_1)\hat{}2\,sin(\alpha_1)\,(sin(\phi)\,sin(\psi) \\ & +\,cos(\phi)\,cos(\psi)\,sin(\theta)))/3 - (16\,a\,cos(\alpha_2)\,cos(\beta_2)\hat{}2\,sin(\alpha_2)\,(sin(\phi)\,sin(\psi) \\ & +\,cos(\phi)\,cos(\psi)\,sin(\theta)))/3 - (16\,a\,cos(\psi)\,cos(\theta)\,cos(\beta_1)\,sin(\alpha_1)\,sin(\beta_1))/3 \\ & -(16\,a\,cos(\psi)\,cos(\theta)\,cos(\beta_2)\,sin(\alpha_2)\,sin(\beta_2))/3\end{aligned}$$

$$\begin{aligned}A_{22} = {} & 6\,\pi r\,(cos(\phi)\,cos(\psi) + sin(\phi)\,sin(\psi)\,sin(\theta)) + (16\,a\,(cos(\phi)\,cos(\psi) \\ & +\,sin(\phi)\,sin(\psi)\,sin(\theta))\,(-\sin^2(\alpha_1)\,\sin^2(\beta_1) + \sin^2(\alpha_1) + 2))/3 \\ & +\,(16\,a\,(cos(\phi)\,cos(\psi) + sin(\phi)\,sin(\psi)\,sin(\theta))\,(-\sin^2(\alpha_2)\sin^2(\beta_2) + \sin^2(\alpha_2) + 2))/3 \\ & +\,(16\,a\,cos(\alpha_1)\,\cos^2(\beta_1)\;\,sin(\alpha_1)\,(cos(\psi)\,sin(\phi) - cos(\phi)\,sin(\psi)\,sin(\theta)))/3 \\ & +\,(16\,a\,cos(\alpha_2)\,cos(\beta_2)\hat{}2\,sin(\alpha_2)\,(cos(\psi)\,sin(\phi) - cos(\phi)\,sin(\psi)\,sin(\theta)))/3 \\ & -(16\,a\,cos(\theta)\,cos(\beta_1)\,sin(\psi)\,sin(\alpha_1)\,sin(\beta_1))/3 \\ & -(16\,a\,cos(\theta)\,cos(\beta_2)\,sin(\psi)\,sin(\alpha_2)\,sin(\beta_2))/3\end{aligned}$$

$$\begin{aligned}A_{23} = {} & (16\,a\,cos(\theta)\,sin(\phi)\,(-sin^2(\alpha_1)\,sin^2(\beta_1) + sin^2(\alpha_1) + 2))/3 \\ & +\,(16\,a\,cos(\theta)\,sin(\phi)\,(-sin^2(\alpha_2)\,sin^2(\beta_2) + sin^2(\alpha_2) + 2))/3 + 6\,\pi r\,cos(\theta)\,sin(\phi) \\ & +\,(16\,a\,cos(\beta_1)\,sin(\theta)\,sin(\alpha_1)\,sin(\beta_1))/3 + (16\,a\,cos(\beta_2)\,sin(\theta)\,sin(\alpha_2)\,sin(\beta_2))/3 \\ & -(16\,a\,cos(\phi)\,cos(\theta)\,cos(\alpha_1)\,cos^2(\beta_1)\,sin(\alpha_1))/3 \\ & -(16\,a\,cos(\phi)\,cos(\theta)\,cos(\alpha_2)\,cos^2(\beta_2)\,sin(\alpha_2))/3\end{aligned}$$

$$A_{24} = 0$$

$$\begin{aligned}A_{25} = {} & (16\,a\,sin(\phi)\,(l+s_2)\,(-sin^2(\alpha_2)\,sin^2(\beta_2) + sin^2(\alpha_2) + 2))/3 \\ & -(16\,a\,sin(\phi)\,(l+s_1)\,(-sin^2(\alpha_1)\,sin^2(\beta_1) + sin^2(\alpha_1) + 2))/3 \\ & +\,(16\,a\,cos(\phi)\,cos(\alpha_1)\,cos^2(\beta_1)\,sin(\alpha_1)\,(l+s_1))/3 \\ & -(16\,a\,cos(\phi)\,cos(\alpha_2)\,cos^2(\beta_2)\,sin(\alpha_2)\,(l+s_2))/3\end{aligned}$$

$$\begin{aligned}A_{26} = {} & (16\,a\,cos(\phi)\,cos(\theta)\,(l+s_1)\,(-sin^2(\alpha_1)\,sin^2(\beta_1) + sin(\alpha_1)\hat{}2 + 2))/3 \\ & -(16\,a\,cos(\phi)\,cos(\theta)\,(l+s_2)\,(-sin^2(\alpha_2)\,sin^2(\beta_2) + sin^2(\alpha_2) + 2))/3 \\ & +\,(16\,a\,cos(\theta)\,sin(\phi)\,cos(\alpha_1)\,cos^2(\beta_1)\,sin(\alpha_1)\,(l+s_1))/3 \\ & -(16\,a\,cos(\theta)\,sin(\phi)\,cos(\alpha_2)\,cos^2(\beta_2)\,sin(\alpha_2)\,(l+s_2))/3\end{aligned}$$

https://doi.org/10.1017/S0263574720001289 Published online by Cambridge University Press

$$
\begin{aligned}
A_{31} &= 6\,\pi r\,(sin(\phi)\,sin(\psi) + cos(\phi)\,cos(\psi)\,sin(\theta)) - (16\,a\,(sin(\phi)\,sin(\psi)\\
&\quad + cos(\phi)\,cos(\psi)\,sin(\theta))\,(-sin^2(\alpha_2)\,sin^2(v22) + sin^2(\alpha_2) + sin^2(\beta_2) - 3))/3\\
&\quad - (16\,a\,(sin(\phi)\,sin(\psi)\\
&\quad + cos(\phi)\,cos(\psi)\,sin(\theta))\,(-sin^2(\alpha_1)\,sin^2(\beta_1) + sin^2(\alpha_1) + sin^2(\beta_1) - 3))/3\\
&\quad + (16\,a\,cos(\alpha_1)\,cos^2(\beta_1)\,sin(\alpha_1)\,(cos(\phi)\,sin(\psi) - cos(\psi)\,sin(\phi)\,sin(\theta)))/3\\
&\quad + (16\,a\,cos(\alpha_2)\,cos^2(\beta_2)\,sin(\alpha_2)\,(cos(\phi)\,sin(\psi) - cos(\psi)\,sin(\phi)\,sin(\theta)))/3\\
&\quad + (16\,a\,cos(\psi)\,cos(\theta)\,cos(\alpha_1)\,cos(\beta_1)\,sin(\beta_1))/3\\
&\quad + (16\,a\,cos(\psi)\,cos(\theta)\,cos(\alpha_2)\,cos(\beta_2)\,sin(\beta_2))/3\\
A_{32} &= (16\,a\,(cos(\psi)\,sin(\phi) - cos(\phi)\,sin(\psi)\,sin(\theta))\,(-sin^2(\alpha_1)\,sin^2(\beta_1) + sin^2(\alpha_1)\\
&\quad + sin^2(\beta_1) - 3))/3 + (16\,a\,(cos(\psi)\,sin(\phi) - cos(\phi)\,sin(\psi)\,sin(\theta))\,(-sin^2(\alpha_2)\,sin^2(\beta_2)\\
&\quad + sin^2(\alpha_2) + sin^2(\beta_2) - 3))/3 - 6\,\pi r\,(cos(\psi)\,sin(\phi) - cos(\phi)\,sin(\psi)\,sin(\theta))\\
&\quad - (16\,a\,cos(\alpha_1)\,cos^2(\beta_1)\,sin(\alpha_1)\,(cos(\phi)\,cos(\psi) + sin(\phi)\,sin(\psi)\,sin(\theta)))/3\\
&\quad - (16\,a\,cos(\alpha_2)\,cos(\beta_2)^2\,sin(\alpha_2)\,(cos(\phi)\,cos(\psi) + sin(\phi)\,sin(\psi)\,sin(\theta)))/3\\
&\quad + (16\,a\,cos(\theta)\,cos(\alpha_1)\,cos(\beta_1)\,sin(\psi)\,sin(\beta_1))/3\\
&\quad + (16\,a\,cos(\theta)\,cos(\alpha_2)\,cos(\beta_2)\,sin(\psi)\,sin(\beta_2))/3\\
A_{33} &= 6\,\pi r\,cos(\phi)\,cos(\theta) - (16\,a\,cos(\phi)\,cos(\theta)\,(-sin^2(\alpha_2)\,sin^2(\beta_2) + sin^2(\alpha_2)\\
&\quad + sin^2(\beta_2) - 3))/3 - (16\,a\,cos(\phi)\,cos(\theta)\,(-sin^2(\alpha_1)\,sin^2(\beta_1) + sin^2(\alpha_1)\\
&\quad + sin^2(\beta_1) - 3))/3 - (16\,a\,cos(\alpha_1)\,cos(\beta_1)\,sin(\theta)\,sin(\beta_1))/3\\
&\quad - (16\,a\,cos(\alpha_2)\,cos(\beta_2)\,sin(\theta)\,sin(\beta_2))/3\\
&\quad - (16\,a\,cos(\theta)\,cos(\alpha_1)\,cos^2(\beta_1)\,sin(\phi)\,sin(\alpha_1))/3\\
&\quad - (16\,a\,cos(\theta)\,cos(\alpha_2)\,cos^2(\beta_2)\,sin(\phi)\,sin(\alpha_2))/3\\
A_{34} &= 0\\
A_{35} &= (16\,a\,cos(\phi)\,(l + s_1)\,(-sin^2(\alpha_1)\,sin^2(\beta_1) + sin^2(\alpha_1) + sin^2(\beta_1) - 3))/3\\
&\quad - (16\,a\,cos(\phi)\,(l + s_2)\,(-sin^2(\alpha_2)\,sin^2(\beta_2) + sin^2(\alpha_2) + sin^2(\beta_2) - 3))/3\\
&\quad + (16\,a\,sin(\phi)\,cos(\alpha_1)\,cos^2(\beta_1)\,sin(\alpha_1)\,(l + s_1))/3\\
&\quad - (16\,a\,sin(\phi)\,cos(\alpha_2)\,cos^2(\beta_2)\,sin(\alpha_2)\,(l + s_2))/3\\
A_{36} &= (16\,a\,cos(\theta)\,sin(\phi)\,(l + s_1)\,(-sin^2(\alpha_1)\,sin^2(\beta_1) + sin^2(\alpha_1) + sin^2(\beta_1) - 3))/3\\
&\quad - (16\,a\,cos(\theta))\,sin(\phi)\,(l + s_2)\,(-sin^2(\alpha_2)\,sin^2(\beta_2) + sin^2(\alpha_2) + sin^2(\beta_2) - 3))/3\\
&\quad - (16\,a\,cos(\phi)\,cos(\theta)\,cos(\alpha_1)\,cos^2(\beta_1)\,sin(\alpha_1)\,(l + s_1))/3\\
&\quad + (16\,a\,cos(\phi)\,cos(\theta)\,cos(\alpha_2)\,cos^2(\beta_2)\,sin(\alpha_2)\,(l + s_2))/3\\
A_{41} &= 0\\
A_{42} &= 0\\
A_{43} &= 0\\
A_{44} &= 8\,\pi r^3 + (64\,a^3)/3\\
A_{45} &= 0\\
A_{46} &= -8\,\pi\,sin(\theta) r^3 - (64\,a^3\,sin(\theta))/3
\end{aligned}
$$

https://doi.org/10.1017/S0263574720001289 Published online by Cambridge University Press

$$
\begin{aligned}
A_{51} = {} & (l+s_2)\,((16\,cos(\alpha_2)\,cos^2(\beta_2)\,sin(\alpha_2)\,a\,(cos(\phi)\,sin(\psi)-cos(\psi)\,sin(\phi)\,sin(\theta)))/3\\
& -(16\,a\,(sin(\phi)\,sin(\psi)+cos(\phi)\,cos(\psi)\,sin(\theta))\,(-sin^2(\alpha_2)\,sin^2(\beta_2)\\
& +\,sin^2(\alpha_2)+sin^2(\beta_2)-3))/3+\,(16\,cos(\psi)\,cos(\theta)\,cos(\alpha_2)\,cos(\beta_2)\,sin(\beta_2)\,a)/3)\\
& -(l+s_1)\,((16\,cos(\alpha_1)\,cos^2(\beta_1)\,sin(\alpha_1)\,a\,(cos(\phi)\,sin(\psi)-cos(\psi)\,sin(\phi)\,sin(\theta)))/3\\
& -(16\,a\,(sin(\phi)\,sin(\psi)+cos(\phi)\,cos(\psi)\,sin(\theta))\,(-sin^2(\alpha_1)\,sin^2(\beta_1)\\
& +\,sin^2(\alpha_1)+sin^2(\beta_1)-3))/3+(16\,cos(\psi)\,cos(\theta)\,cos(\alpha_1)\,cos(\beta_1)\,sin(\beta_1)\,a)/3)\\
A_{52} = {} & (l+s_2)\,((16\,a\,(cos(\psi)\,sin(\phi))-cos(\phi)\,sin(\psi)\,sin(\theta))\,(-sin^2(\alpha_2)\,sin^2(\beta_2)\\
& +\,sin^2(\alpha_2)+sin^2(\beta_2)-3))/3-(16\,cos(\alpha_2)\,cos^2(\beta_2)\,sin(\alpha_2)\,a\,(cos(\phi)\,cos(\psi)\\
& +\,sin(\phi)\,sin(\psi)\,sin(\theta)))/3+(16\,cos(\theta)\,cos(\alpha_2)\,cos(\beta_2)\,sin(\psi)\,sin(\beta_2)\,a)/3)\\
& -(l+s_1)\,((16\,a\,(cos(\psi)\,sin(\phi)-cos(\phi)\,sin(\psi)\,sin(\theta))\,(-sin^2(\alpha_1)\,sin^2(\beta_1)\\
& +\,sin^2(\alpha_1)+\,sin^2(\beta_1)-3))/3-(16\,cos(\alpha_1)\,cos^2(\beta_1)\,sin(\alpha_1)\,a\,(cos(\phi)\,cos(\psi)\\
& +\,sin(\phi)\,sin(\psi)\,sin(\theta)))/3+(16\,cos(\theta)\,cos(\alpha_1)\,cos(\beta_1)\,sin(\psi)\,sin(\beta_1)\,a)/3)\\
A_{53} = {} & (l+s_1)\,((16\,cos(\phi)\,cos\,(\theta)\;a\,(-sin^2(\alpha_1)\,sin^2(\beta_1)+sin^2(\alpha_1)+sin^2(\beta_1)-3))/3\\
& +\,(16\,cos(\alpha_1)\,cos(\beta_1)\,sin(\theta)\,sin(\beta_1)\,a)/3\\
& +\,(16\,cos(\theta)\,cos(\alpha_1)\,cos^2(\beta_1)\,sin(\phi)\,sin(\alpha_1)\,a)/3)\\
& -(l+s_2)\,((16\,cos(\phi)\,cos(\theta)\,a\,(-sin^2(\alpha_2)\,sin^2(\beta_2)\\
& +\,sin^2(\alpha_2)+sin^2(\beta_2)-3))/3+(16\,cos(\alpha_2)\,cos(\beta_2)\,sin(\theta)\,sin(\beta_2)\,a)/3\\
& +\,(16\,cos(\theta)\,cos(\alpha_2)\,cos^2(\beta_2)\,sin(\phi)\,sin(\alpha_2)\,a)/3)\\
A_{54} = {} & 0\\
A_{55} = {} & 64\,a^3\,cos(\phi))/3-(l+s_2)\,((16\,a\,cos(\phi)\,(l+s_2)\,(-sin^2(\alpha_2)\,sin^2(\beta_2)+sin^2(\alpha_2)\\
& +\,sin^2(\beta_2)-3))/3+(16\,cos(\alpha_2)\,cos^2(\beta_2)\,sin(\alpha_2)\,a\,sin(\phi)\,(l+s_2))/3)\\
& -(l+s_1)\,((16\,a\,cos(\phi)\,(l+s_1)\,(-sin^2(\alpha_1)\,sin^2(\beta_1)\\
& +\,sin^2(\alpha_1)+sin^2(\beta_1)-3))/3+(16\,cos(\alpha_1))\,cos^2(\beta_1)\,sin(\alpha_1)\,a\,sin(\phi)\,(l+s_1))/3)\\
& +\,8\,\pi\;\,r^3\,cos(\phi)\\
A_{56} = {} & (64\,a^3\,cos(\theta)\,sin(\phi))/3-(l+s_2)\,((16\,a\,cos(\theta)\,sin(\phi)\,(l+s_2)\,(-sin^2(\alpha_2)\,sin^2(\beta_2)\\
& +\,sin^2(\alpha_2)+sin^2(\beta_2)-3))/3-(16\,cos(\alpha_2)\,cos^2(\beta_2)\,sin(\alpha_2)\,a\,cos(\phi)\,cos(\theta)\,(l+s_2))/3)\\
& -(l+s_1)\,((16\,a\,cos(\theta)\,sin(\phi)\,(l+s_1)\,(-sin^2(\alpha_1)\,sin^2(\beta_1)+\,sin^2(\alpha_1)\\
& +\,sin^2(\beta_1)-3))/3-(16\,cos(\alpha_1)\,cos^2(\beta_1)\,sin(\alpha_1)\,a\,cos(\phi)\,cos(\theta)\,(l+s_1))/3)\\
& +\,8\,\pi r^3\,cos(\theta)sin(\phi)\\
A_{61} = {} & (l+s_2)\,((16\,a\,(cos(\phi)\,sin(\psi)-cos(\psi)\,sin(\phi)\,sin(\theta))\,(-sin^2(\alpha_2)\,sin^2(\beta_2)\\
& +\,sin^2(\alpha_2)+2))/3+(16\,cos(\alpha_2)\,cos^2(\beta_2)\,sin(\alpha_2)\,a\,(sin(\phi)\,sin(\psi)\\
& +\,cos(\phi)\,cos(\psi)\,sin(\theta)))/3+(16\,cos(\psi)\,cos(\theta)\,cos(\beta_2)\,sin(\alpha_2)\,sin(\beta_2)\,a)/3)\\
& -(l+s_1)\,((16\,a\,(cos(\phi)\,sin(\psi)-cos(\psi)\,sin(\phi)\,sin(\theta))\,(-sin^2(\alpha_1)\,sin^2(\beta_1)\\
& +\,sin^2(\alpha_1)+2))/3+(16\,cos(\alpha_1)\,cos^2(\beta_1)\,sin(\alpha_1)\,a\,(sin(\phi)\,sin(\psi)\\
& +\,cos(\phi)\,cos(\psi)\,sin(\theta)))/3+(16\,cos(\psi)\,cos(\theta)\,cos(\beta_1)\,sin(\alpha_1)\,sin(\beta_1)\,a)/3)
\end{aligned}
$$

https://doi.org/10.1017/S0263574720001289 Published online by Cambridge University Press

$$
\begin{aligned}
A_{62} = {} & (l+s_1)\,((16\,a\,(cos(\phi)\,cos(\psi)+sin(\phi)\,sin(\psi)\,sin(\theta))\,(-sin^2(\alpha_1)\,sin^2(\beta_1)\\
& +\ sin^2(\alpha_1)+2))/3+(16\,cos(\alpha_1)\,cos^2(\beta_1)\,sin(\alpha_1)\,a\,(cos(\psi)\,sin(\phi)\\
& -cos(\phi)\,sin(\psi)\,sin(\theta)))/3-(16\,cos(\theta)\,cos(\beta_1)\,sin(\psi)\,sin(\alpha_1)\,sin(\beta_1)\,a)/3)\\
& -(l+s_2)\,((16\,a\,(cos(\phi)\,cos(\psi)+sin(\phi)\,sin(\psi)\,sin(\theta))\,(-sin^2(\alpha_2)\,sin^2(\beta_2)\\
& +\ sin^2(\alpha_2)+2))/3+(16\,cos(\alpha_2)\,cos^2(\beta_2)\,sin(\alpha_2)\,a\,(cos(\psi)\,sin(\phi)\\
& -cos(\phi)\,sin(\psi)\,sin(\theta)))/3-(16\,cos(\theta)\,cos(\beta_2)\,sin(\psi)\,sin(\alpha_2)\,sin(\beta_2)\,a)/3)\\
A_{63} = {} & (l+s_1)\,((16\,cos(\theta)\,sin(\phi)\,a\,(-sin^2(\alpha_1)\,sin^2(\beta_1)+sin^2(\alpha_1)+2))/3\\
& +(16\,cos(\beta_1)\,sin(\theta)\,sin(\alpha_1)\,sin(\beta_1)\,a)/3\\
& -(16\,cos(\phi)\,cos(\theta)\,cos(\alpha_1)\,cos^2(\beta_1)\,sin(\alpha_1)\,a)/3)\\
& -(l+s_2)\,((16\,cos(\theta)\,sin(\phi)\,a\,(-sin^2(\alpha_2)\,sin^2(\beta_2)+sin^2(\alpha_2)+2))/3\\
& +\ (16\,cos(\beta_2)\,sin(\theta)\,sin(\alpha_2)\,sin(\beta_2)\,a)/3\\
& -(16\,cos(\phi)\,cos(\theta)\,cos(\alpha_2)\,cos^2(\beta_2)\,sin(\alpha_2)\,a)/3)\\
A_{64} = {} & 0\\
A_{65} = {} & -8\pi\,sin(\phi)r^3-(64\,a^3\,sin(\phi))/3-(l+s_1)\,((16\,a\,sin(\phi)\,(l+s_1)\,(-sin^2(\alpha_1)\,sin^2(\beta_1)\\
& +\ sin^2(\alpha_1)+2))/3-(16\,cos(\alpha_1)\,cos^2(\beta_1)\,sin(\alpha_1)\,a\,cos(\phi)\,(l+s_1))/3)\\
& -(l+s_2)\,((16\,a\,sin(\phi)\,(l+s_2)\,(-sin(\alpha_2)\hat{}2\,sin^2(\beta_2)+sin^2(\alpha_2)+2))/3\\
& -(16\,cos(\alpha_2)\,cos^2(\beta_2)\,sin(\alpha_2)\,a\,cos(\phi)\,(l+s_2))/3)\\
A_{66} = {} & (l+s_1)\,((16\,a\,cos(\phi)\,cos(\theta)\,(l+s_1)\,(-sin^2(\alpha_1)\,sin^2(\beta_1)+sin^2(\alpha_1)+2))/3\\
& +\ (16\,cos(\alpha_1)\,cos^2(\beta_1)\,sin(\alpha_1)\,a\,cos(\theta)\,sin(\phi)\,(l+s_1))/3)\\
& +\ (l+s_2)\,((16\,a\,cos(\phi)\,cos(\theta)\,(l+s_2)\,(-sin^2(\alpha_2)\,sin^2(\beta_2)+sin^2(\alpha_2)+2))/3\\
& +(16\,cos(\alpha_2)\,cos^2(\beta_2)\,sin(\alpha_2)\,a\,cos(\theta)\,sin(\phi)\,(l+s_2))/3)\\
& +\ (64\,a^3\,cos(\phi)\,cos(\theta))/3+8\,\pi r^3\,cos(\phi)\,cos(\theta)
\end{aligned}
$$

The B matrix parameters in Eq. (16) are defined as followed:

$$
\begin{aligned}
B_{11} &= (16\,a\,(sin^2(\beta_1)+2))/3\\
B_{12} &= -(16\,a\,(sin^2(\beta_2)+2))/3\\
B_{13} &= 0\\
B_{14} &= 0\\
B_{21} &= -(16\,a\,cos(\beta_1)\,sin(\alpha_1)\,sin(\beta_1))/3\\
B_{22} &= (16\,a\,cos(\beta_2)\,sin(\alpha_2)\,sin(\beta_2))/3\\
B_{23} &= 0\\
B_{24} &= 0\\
B_{31} &= (16\,a\,cos(\alpha_1)\,cos(\beta_1)\,sin(\beta_1))/3\\
B_{32} &= -(16\,a\,cos(\alpha_2)\,cos(\beta_2)\,sin(\beta_2))/3\\
B_{33} &= 0\\
B_{34} &= 0\\
B_{41} &= 0\\
B_{42} &= 0\\
B_{43} &= 0
\end{aligned}
$$

https://doi.org/10.1017/S0263574720001289 Published online by Cambridge University Press

$$B_{44} = 0$$
$$B_{51} = -(16\, cos(\alpha_1)\, cos(\beta_1)\, sin(\beta_1)\, a\, (l + s_1))/3$$
$$B_{52} = -(16\, cos(\alpha_2)\, cos(\beta_2)\, sin(\beta_2)\, a\, (l + s_2))/3$$
$$B_{53} = (32\, a^3\, cos(\alpha_1))/3$$
$$B_{54} = (32\, a^3\, cos(\alpha_2))/3$$
$$B_{61} = -(16\, cos\, (\beta_1)\ \ sin\, (\alpha_1)\ \ sin\, (\beta_1)\ \ a(l + s_1))/3$$
$$B_{62} = -(16\, cos(\beta_2)\, sin(\alpha_2)\, sin(\beta_2)\, a(l + s_2))/3$$
$$B_{63} = -(32\, a^3\, sin(\alpha_1))/3$$
$$B_{64} = -(32\, a^3\, sin(\alpha_2))/3$$

https://doi.org/10.1017/S0263574720001289 Published online by Cambridge University Press